

Comparison of the Predicted and Measured Loss Factor of the Superconducting Cavity Assembly for the CESR Upgrade*

S. Belomestnykh[†], W. Hartung, J. Kirchgessner, D. Moffat, H. Muller, H. Padamsee, and V. Veshcherevich[†]

Laboratory of Nuclear Studies, Cornell University, Ithaca, NY 14853 USA

Abstract

The loss factor of the superconducting cavity module for the CESR upgrade has been measured in a beam test for bunch lengths between 10 and 25 mm, using a calorimetric method. The data are compared with predictions from the ABCI and TBCI computer codes (for the cavity module) and from the AMOS code and analytic formulae (for the ferrite HOM load). The agreement is quite good. Possible sources of discrepancy are discussed. We also describe an improved HOM load design and report on the results of a high power test on one of these loads.

I. INTRODUCTION

Superconducting cavities have been chosen to replace the existing copper cavities for the future upgrade of CESR. The use of superconducting cavity modules, specially designed for a high current collider, allows us to lower the cavity impedance and the loss factor of the accelerating system and thereby increase the threshold for multi- and single-bunch instabilities [1, 2]. The prototype superconducting cavity assembly was developed at the Laboratory of Nuclear Studies, Cornell University [3, 4] and successfully tested recently in a beam test in the CESR storage ring [5].

Figure 1 shows a schematic of the entire module which includes the cavity, a 24 cm round beam pipe, a fluted beam pipe, a ferrite HOM loads, sliding joints, gate valves and tapers to the CESR beam pipe.

The beam tubes were designed so that all of the higher order modes (HOMs) propagate out of the cavity and are damped by ferrite HOM loads which are located outside the cryostat and which are an integral part of the beam tube.

Systematic studies were done to estimate the interaction of a bunched beam with the cavity module, including the HOM load [6, 7]. ABCI, TBCI and AMOS were used to calculate the loss factor as a function of bunch length. Also, an analytical approach was developed to estimate the coupling impedance and loss factor of the HOM loads.

The loss factor was measured in the beam test using a calorimetric method; we measured the temperature rise and flow rate of the cooling water for the HOM load. To measure the loss factor vs. bunch length (10 to 25 mm), we used two different sets of CESR optics and different RF voltages. The experimental data points are in a good agreement with predicted values.

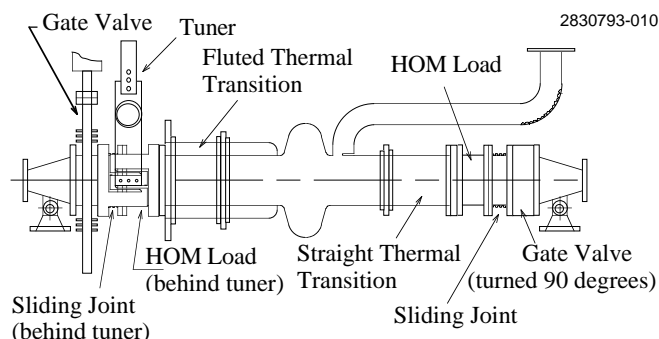


Figure 1. Schematic of the SRF cavity module.

II. HOM LOADS

In the high power RF test of the first HOM load prototype [8], several ferrite tiles cracked. Subsequent examination revealed that the solder bond between the ferrite and the tin-plated stainless steel shell was poor. The HOM load was therefore redesigned. A new, so-called “porcupine” load was developed (see Figures 2 and 3). It consists of a stainless steel shell with 18 copper plates bolted along the inside. Each copper plate carries two 2" long or four 1" long soldered TT-111R ferrite tiles¹. The tiles are 1.5" wide and 0.125" thick. Copper tubing is brazed to each plate for water cooling. This modular design is more tolerant of soldering problems than its predecessor.

Three loads have been fabricated. We used two of them in the beam test. The third was subjected to a separate high power test. An inner conductor was placed concentric to the HOM load and the assembly was connected to 50 Ohm

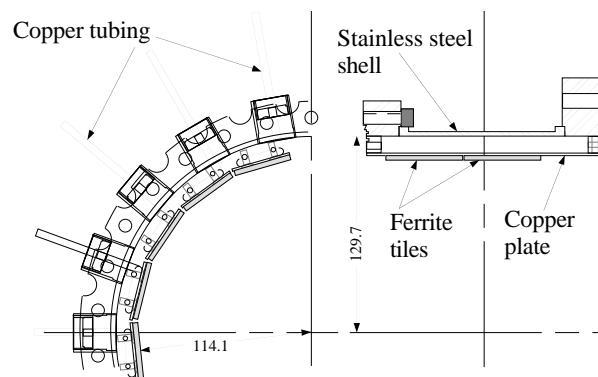


Figure 2. Design of the porcupine HOM load.

* Work supported by National Science Foundation, with supplementary support from the US-Japan Collaboration.

[†] Visitor from Budker Institute of Nuclear Physics, 630090 Novosibirsk, Russia

¹Product of Trans-Tech Inc., Adamstown, MD

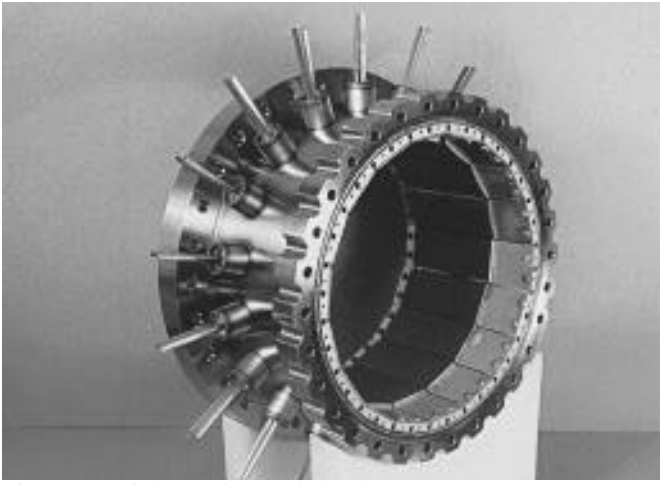


Figure 3. Higher order mode load.

coaxial line terminated by 30 kW water load (see Figure 4). We used a 500 MHz klystron as a source of RF power. The dissipated power was measured via RF (directional couplers) and calorimetry (temperature rise and flow rate of the cooling water). Tile surface temperature measurements were done with “button” type temperature-indicating labels. The test load reached an average power density of 20 W/cm^2 at which point the maximum measured surface temperatures were in excess of 150°C , and the water ΔT was 55°C at a flow rate of 0.9 gpm. The test was done in air, not in vacuum. The agreement between the RF and calorimetric measurements of the dissipated power is quite good (Figure 5).

III. CALCULATIONS OF THE LOSS FACTOR

One can calculate the loss factor of an axially symmetric accelerating structure using TBCI [9] or ABCI [10, 11]. Unfortunately, these programs do not allow us to calculate wake fields in the presence of absorbing materials such as ferrite. On the other hand, AMOS [12] can handle such materials but we have not yet successfully applied it to complex geometries. In the mean time we are using a palliative measure: we calculate the loss factor of the simplified geometry (not taking into account the RF coupler and flutes) of the cavity module without ferrite and of the

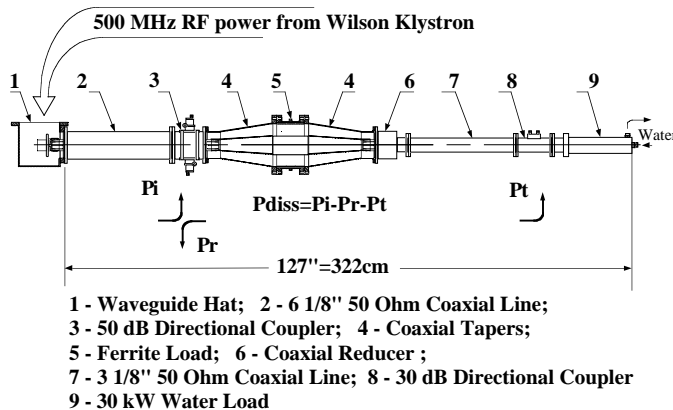


Figure 4. Layout of the HOM load high power test.

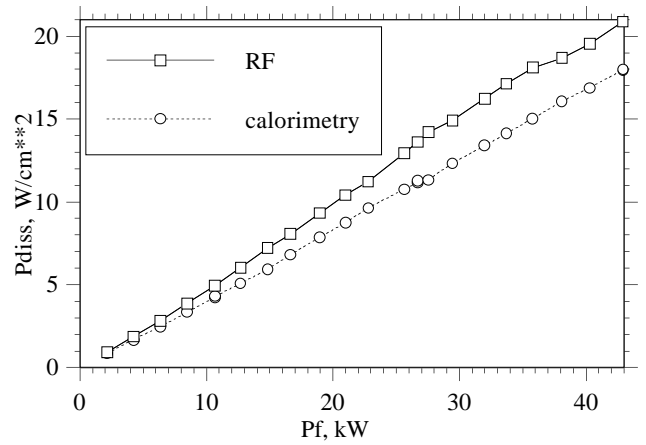


Figure 5. Comparison of RF and calorimetric data from the HOM load high power test.

ferrite load alone, adding the results to get the total loss factor of the assembly. As an alternative to AMOS, we also used an analytical approach [7].

A. The Loss Factor of the Cavity Module

Initial calculations of the loss factor for the cavity module were done using TBCI [6]. The RF coupler, the flutes on one of the beam tubes, and the ferrite were not taken into account. Moreover, the cavity module had to taper to two different beam pipe cross-sections, because of variation in the CESR vacuum chamber dimensions. We averaged TBCI results for bunches travelling in each direction to obtain the “irreversible” contribution. We found that the cavity's loss factor is larger than that of the tapers for long bunches ($\sigma_l > 1.4 \text{ cm}$), but smaller for short bunches.

We did further calculations with ABCI, the latest version of which has such advantages as a moving mesh, an improved method for calculating the wake potentials, and variable radial mesh size. ABCI results for the geometry used in [6] are consistent with the TBCI results.

B. The Loss Factor of the HOM Load

As mentioned above, the new HOM loads have ferrite tiles attached to copper plates which are placed at a slightly smaller radius than that of the beam tube. At present AMOS deals only with the axisymmetric case in which the lossy material fills an outward protrusion in the beam pipe, therefore we used the modified geometry shown in Figure 6 for the calculation.

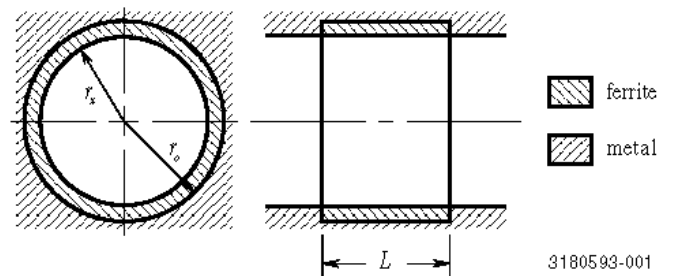


Figure 6. Simplified geometry of the porcupine HOM load for AMOS calculations: $L = 101.6 \text{ mm}$, $r_x = 114.0968 \text{ mm}$, and $r_o = 117.2718 \text{ mm}$.

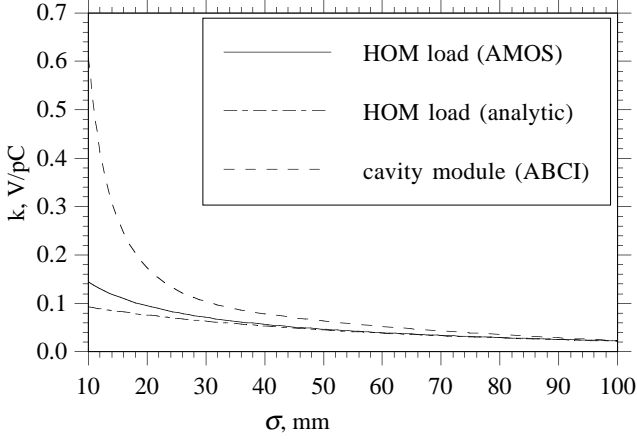


Figure 7. The calculated loss factor of the cavity module (ABCI), and HOM load (AMOS and analytical) as a function of bunch length.

The predicted loss factors for the cavity module (ABCI) and the HOM load (AMOS and analytical) are shown in Figure 7.

IV. LOSS FACTOR MEASUREMENTS IN A BEAM TEST

We measured the temperature of the input and output cooling water for each HOM load, along with the water flow rate. The values yield the power transferred to the water from the ferrite:

$$P = \sum_{i=1}^2 v_f^i C \rho (T_{out}^i - T_{in}^i),$$

where P is the power transferred to the cooling water from the two HOM loads; v_f is the water flow rate; C is the specific heat capacity of the water; ρ is the water density; T_{out} and T_{in} are the output and input temperatures of the cooling water.

This power should be approximately equal to the power lost by the beam due to its interaction with the cavity structure below the cutoff frequencies of the beam pipes because (i) in our HOM load design (Figure 2) other heat transfer mechanisms (conduction through the copper plate to the stainless steel shell, and heat radiation) should not give a significant contribution in comparison with water cooling, and (ii) the HOMs with resonant frequencies below the cutoff frequencies of the nearby beam pipes (2.2 GHz and 3.4 GHz) are trapped inside the accelerating structure, so all their energy should be dissipated in the lossy material of the HOM loads.

We used two different sets of CESR optics to obtain bunch lengths between 10 and 25 mm. Some machine parameters for these optics are given in Table 1. Uniformly-filled bunches were used. Most measurements were done with one bunch or 9 bunches. For uniformly-filled bunches, the loss factor is given by

$$k = \frac{N P f_{rev}}{I_o^2},$$

where I_o is the average beam current; f_{rev} is the revolution frequency; N is the number of bunches.

Table 1. Selected Parameters of the CESR Storage Ring

Parameter	High Energy Lattice	Low Energy Lattice
Revolution frequency	390.14788 kHz	
Beam energy	5.265 GeV	4.400 GeV
SR energy loss per turn	1.0105 MeV	0.4928 MeV
Momentum compaction	0.01142	0.00926
Energy spread	$6.122 \cdot 10^{-4}$	$5.116 \cdot 10^{-4}$

We do not have a bunch length monitor for CESR, but previous measurements [13, 14] indicate that there is no bunch lengthening in the storage ring; so we can calculate the bunch length via

$$\sigma_l = \frac{\alpha c}{\Omega_s} \cdot \frac{\sigma_E}{E_o},$$

$$\Omega_s^2 = \omega_{rev}^2 \cdot \frac{\alpha h e \sqrt{V_{RF}^2 - (U_o/e + U_{coh}/e)^2}}{2\pi E_o},$$

where α is the momentum compaction factor; c is the speed of light; Ω_s is the synchrotron frequency; σ_E is the energy spread; h is the RF harmonic number, E_o is the beam energy; V_{RF} is the RF voltage; U_o is the energy loss per turn due to synchrotron radiation; and U_{coh} is the coherent energy loss per turn due to the total loss factor of the ring.

To verify that we do not have bunch lengthening, the loss factor was plotted as function of beam current for the same machine optics (high energy lattice) and RF voltage (Figures 8, 9). The theoretical bunch length σ_l is equal to 15.3 mm for these measurements. One can see that the loss factor does not depend on current, i.e. there is no evidence of the bunch lengthening.

The experimental results for the loss factor versus bunch length are compared with the predictions in Figure 10. One can see that there is some disagreement for the shortest bunch length. That disagreement may be due to propagation of some portion of the HOM power into the beam pipes for frequencies above cutoff. Also, there is a big disagreement for the 25 mm bunch length. That data point was obtained with the low-energy CESR lattice, using only the SRF voltage (the CESR NRF system was switched off and the NRF cavities were detuned). Unfortunately, the accelerating voltage was not high enough to allow us make measurements with high beam current: the total current was limited to 29 mA in 9 bunches due to poor life time. Therefore the signal was small and this data point may have a big systematic error.

V. CONCLUSIONS

The calorimetric method was successfully applied to measure the loss factor of the superconducting cavity assembly in the CESR beam test. The results are consistent with predicted values.

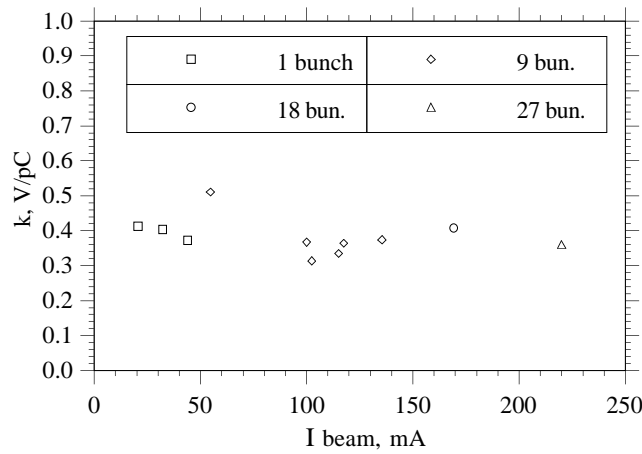


Figure 8. The loss factor of the SRF cavity vs. total beam current.

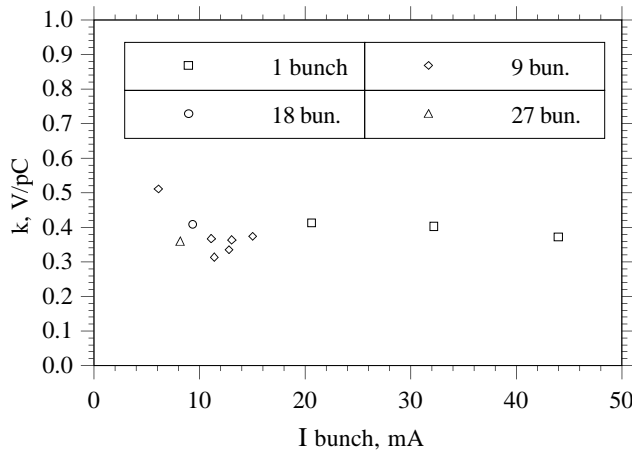


Figure 9. The loss factor of the SRF cavity vs. current per bunch.

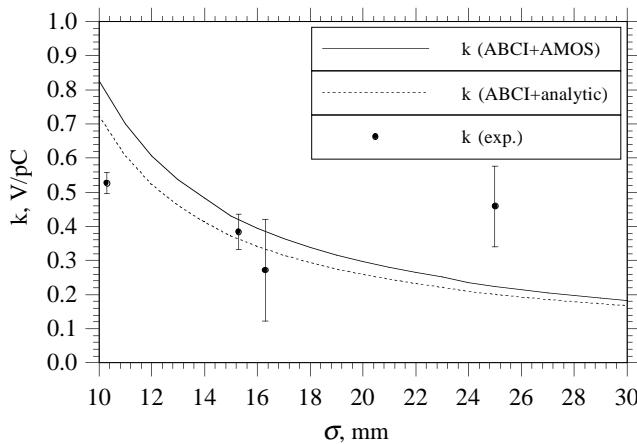


Figure 10. The loss factor of the SRF cavity assembly (experimental data and prediction).

VI. REFERENCES

- [1] H. Padamsee, et al., "Accelerating Cavity Development for the Cornell B-Factor, CESR-B", *Conference Record of the 1991 Particle Accelerator Conference*, Vol. 2, pp. 786-788, San Francisco, CA, May 1991
- [2] H. Padamsee, et al., "Design Challenges for High Current Storage Rings", *Particle Accelerators*, 1992, Vol. 40, pp. 17-41
- [3] D. Moffat, et al., "Preparation and Testing of a Superconducting Cavity for CESR-B", *Proceedings of the 1993 Particle Accelerator Conference*, Vol. 2, pp. 763-765, Washington, D.C., May 1993
- [4] H. Padamsee, et al., "Development and Test of a Superconducting Cavity for High Current Electron Storage Rings", *Proceedings of the Fourth European Particle Accelerator Conference*, Vol. 3, pp. 2048-2050, London, Great Britain, June 1994
- [5] H. Padamsee, et al., "Beam Test of a Superconducting Cavity for the CESR Luminosity Upgrade", *these proceedings*
- [6] V. Veshcherevich, et al., "The Loss Factor of the Cavity Module for the CESR Beam Test and Some Other Asymmetric Structures", *SRF-931013/11*, Laboratory of Nuclear Studies, Cornell University (October 1993)
- [7] W. Hartung, et al., "The Interaction of a Beam with a Beam Line High-Order Mode Absorber", *Proceedings of the 1993 Particle Accelerator Conference*, Vol. 2, pp. 3450-3452, Washington, D.C., May 1993
- [8] D. Moffat, et al., "Design and Fabrication of a Ferrite-lined HOM Load for CESR-B", *Proceedings of the 1993 Particle Accelerator Conference*, Vol. 2, pp. 977-979, Washington, D.C., May 1993
- [9] T. Weiland, "Transverse Beam Cavity Interaction, Part I: Short Range Forces", *DESY 82-015*, Deutsches Elektronen Synchrotron, Hamburg, Germany (March 1982)
- [10] Y. H. Chin, "Advances and Applications of ABCI", *Proceedings of the 1993 Particle Accelerator Conference*, Vol. 2, pp. 3414-3416, Washington, D.C., May 1993
- [11] Y. H. Chin, "User's Guide for ABCI. Version 8.7 (Azimuthal Beam Cavity Interactions)", *LBL-35258, CBP Note-069, CERN SL/94-02 (AP)*
- [12] J. DeFord, et al., "The AMOS (Azimuthal Mode Simulator) Code", *Proceedings of the 1989 IEEE Particle Accelerator Conference*, Vol. 2, pp. 1181-1183, Chicago, IL, March 1989
- [13] E. B. Blum, et al., "Bunch Length Measurements in CESR Using an X-Ray Sensitive Photoconducting Detector", *Nuclear Instruments and Methods*, 1983, Vol. 207, pp. 321-324
- [14] Z. Greenwald, et al., "Bunch Length Measurement Using Beam Spectrum", *Conference Record of the 1991 Particle Accelerator Conference*, Vol. 2, pp. 1246-1248, San Francisco, CA, May 1991